

Controlling synchronization dynamics via physics-informed neural networks

Kaiming Luo

School of Information Science and Technology, Fudan University, Shanghai 200438, China

(Dated: January 5, 2026)

Synchronization control in networked dynamical systems requires regulating not only whether coherence is achieved, but also when and to what extent it emerges. We propose a physics-informed neural network (PINN) framework for continuous-time synchronization regulation, in which system trajectories and control inputs are jointly parameterized and constrained by the governing dynamics. Macroscopic synchronization objectives are imposed directly at the trajectory level by enforcing persistence conditions on the order parameter after a prescribed target time. This formulation enables simultaneous control of synchronization time and coherence level without assuming any explicit feedback law or solving a strict optimal control problem. Numerical studies on networked Kuramuro oscillators demonstrate smooth synchronization with reduced transient control effort and competitive cumulative cost relative to analytical baselines. The framework remains effective in non-gradient and frustrated dynamics, highlighting physics-informed neural control as a flexible trajectory-level approach to synchronization regulation.

I. INTRODUCTION

Synchronization is one of the most fundamental collective phenomena in nonlinear dynamics and complex systems, arising ubiquitously in physical, chemical, biological, and engineering contexts [1, 2]. Examples range from Josephson junction arrays [3] and laser networks [4] to neuronal populations [5] and power grids [6], where mutual coupling among individual units leads to the emergence of coherent phase or frequency dynamics. The degree of synchronization often plays a decisive role in determining the macroscopic functionality and stability of such systems [7]. As a result, the regulation of synchronization processes has long been a central topic in the study of complex dynamical systems [8].

In many practical situations, synchronization is not merely a binary property indicating whether coherence is present or absent, but rather a dynamical process that can, in principle, be regulated [9]. On the one hand, it is often desirable for a system to reach a synchronized state within a finite time window, in order to avoid prolonged desynchronization and the associated degradation of performance or stability [10, 11]. On the other hand, different applications may require different levels of coherence, ranging from partial synchronization to strong phase locking or near-complete synchrony [12–14]. From this perspective, a physically meaningful control problem is to regulate both the time scale over which synchronization emerges and the degree of coherence ultimately attained, subject to the constraints imposed by the underlying dynamics [15, 16].

A variety of control strategies have been proposed to influence synchronization processes in nonlinear networks, including phase-feedback control, pinning control, and other structured control schemes [17–19]. While these approaches can be effective under specific assumptions, they typically rely on prescribed control laws or local linearization arguments [20, 21]. As a consequence, synchronization performance—including the achieved coherence level, convergence time, and control effort—is

usually assessed a posteriori, rather than being specified directly at the trajectory level. This limitation becomes particularly pronounced in high-dimensional, strongly nonlinear, or heterogeneous systems, where shaping the full temporal evolution of collective dynamics remains challenging [22–24].

In recent years, physics-informed neural networks (PINNs) have emerged as a powerful approach for learning and controlling dynamical systems under physical constraints [25, 26]. By embedding governing equations directly into the training process of neural networks, PINNs ensure that learned trajectories remain consistent with known physical laws [27]. This property makes PINNs particularly attractive for continuous-time problems, where explicit time discretization may introduce numerical stiffness or limit flexibility in trajectory design [28]. PINNs have been successfully applied to a wide range of problems, including system identification, inverse problems, and constrained trajectory learning [25, 29].

Building on these developments, PINNs offer a natural framework for synchronization regulation, in which both system trajectories and control inputs can be represented in a unified, physics-constrained manner [30]. By incorporating system dynamics, initial conditions, and synchronization objectives into a single continuous-time optimization problem, collective observables such as order parameters can be regulated directly at the trajectory level [31]. Importantly, this perspective shifts the focus away from prescribing explicit feedback laws or solving optimal control problems in a strict sense, and instead toward discovering admissible and energy-efficient control trajectories that satisfy physical constraints while achieving desired collective behaviors [32].

Motivated by these considerations, we develop a physics-informed neural control framework for the continuous-time regulation of synchronization in networked dynamical systems. The approach reformulates synchronization control as a trajectory-level optimization problem, in which system dynamics, macroscopic

synchronization requirements, and control regularization are enforced simultaneously. This formulation allows the synchronization level and the time at which it must be reached to be specified explicitly, without assuming any predefined feedback structure. Using networks of coupled oscillators as a representative testbed, we systematically analyze how the control effort depends on intrinsic dynamical parameters and synchronization targets, and benchmark the learned control in analytically solvable synchronization models, exemplified by the Kuramoto model, where synchronization dynamics and low-energy control strategies admit explicit analytical characterization. The framework further remains effective in non-gradient settings where conventional analytical controls break down, highlighting its generality as a physics-constrained approach to synchronization regulation.

II. PHYSICS-INFORMED NEURAL CONTROL FRAMEWORK

We consider a general class of continuous-time controlled dynamical systems governed by

$$\dot{\mathbf{x}}(t) = \mathbf{f}(\mathbf{p}, \mathbf{x}(t), \mathbf{u}(t)), \quad (1)$$

where $\mathbf{x}(t) \in \mathbb{R}^d$ denotes the system state at time t , $\mathbf{u}(t) \in \mathbb{R}^m$ represents an external control input, and \mathbf{p} is a collection of fixed system parameters, such as coupling strengths or network structure. The nonlinear vector field \mathbf{f} encodes the intrinsic dynamics of the system as well as the manner in which control inputs enter the evolution. The objective of synchronization regulation is not merely to determine whether coherent behavior emerges, but to shape the temporal evolution of collective dynamics generated by Eq. (1).

The proposed framework represents both the state trajectory $\mathbf{x}(t)$ and the control input $\mathbf{u}(t)$ using neural networks, while enforcing the governing dynamics as physics-informed constraints. As illustrated in Fig. 1, time t is used as the sole explicit input to a feedforward neural network with multiple hidden layers. The network produces two outputs, denoted by $N_x(t)$ and $N_u(t)$, which parameterize the state evolution and control signal, respectively. This joint representation enables the system trajectory and the control input to be learned simultaneously within a unified architecture.

To ensure exact satisfaction of the initial conditions for both the system state and the control input, the neural network outputs are incorporated through the parametrization

$$\begin{aligned} \mathbf{x}(t) &= \mathbf{x}(0) + h(t) N_x(t), \\ \mathbf{u}(t) &= \mathbf{u}(0) + h(t) N_u(t), \end{aligned} \quad (2)$$

where $\mathbf{x}(0)$ denotes the prescribed initial state and $\mathbf{u}(0)$ denotes the initial control value. The function $h(t)$ is a smooth shaping function satisfying $h(0) = 0$, which guarantees that both $\mathbf{x}(t)$ and $\mathbf{u}(t)$ exactly satisfy their

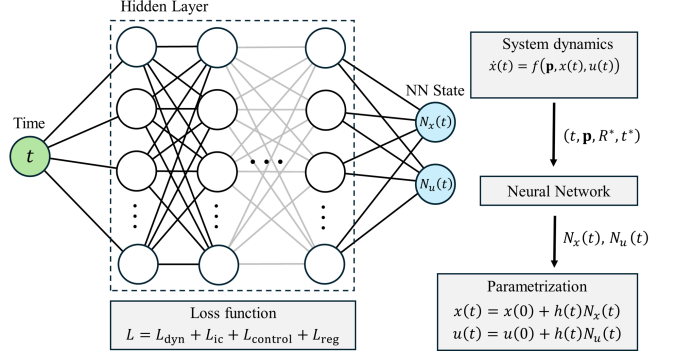


FIG. 1. Schematic illustration of the physics-informed neural control framework. Time t is used as the input to a neural network with multiple hidden layers, which jointly outputs a state network $N_x(t)$ and a control network $N_u(t)$. These outputs are combined with a shaping function $h(t)$ to parameterize the system state $\mathbf{x}(t)$ and control input $\mathbf{u}(t)$ while exactly enforcing the initial condition. The governing system dynamics $\dot{\mathbf{x}}(t) = \mathbf{f}(\mathbf{p}, \mathbf{x}(t), \mathbf{u}(t))$ are incorporated through physics-informed residuals, and training is performed by minimizing a composite loss function consisting of dynamical, initial-condition, control, and regularization terms.

respective initial conditions at $t = 0$. This construction, shown schematically in Fig. 1, allows the neural networks to flexibly represent admissible state trajectories and control profiles for $t > 0$, while preserving consistency with the specified initial conditions.

Consistency between the neural-network parameterized trajectories and the underlying dynamics is enforced by penalizing the residual of Eq. (1). Specifically, the physics-informed residual is defined as

$$\mathbf{r}(t) = \frac{d\mathbf{x}(t)}{dt} - \mathbf{f}(\mathbf{p}, \mathbf{x}(t), \mathbf{u}(t)), \quad (3)$$

where the time derivative $d\mathbf{x}(t)/dt$ is computed via automatic differentiation of the neural network output. Evaluating and penalizing the residual $\mathbf{r}(t)$ at a set of collocation points in time constrains the learned trajectories to remain consistent with the prescribed system dynamics, as conceptually indicated by the feedback between the neural network and the dynamical equation in Fig. 1. Training of the neural networks is carried out by minimizing a composite loss function of the form

$$\mathcal{L} = \mathcal{L}_{\text{dyn}} + \mathcal{L}_{\text{ic}} + \mathcal{L}_{\text{control}} + \mathcal{L}_{\text{reg}}, \quad (4)$$

where \mathcal{L}_{dyn} penalizes the mean-squared physics-informed residual defined in Eq. (3), \mathcal{L}_{ic} enforces the initial condition through Eq. (2), $\mathcal{L}_{\text{control}}$ encodes the synchronization objective, and \mathcal{L}_{reg} represents the cost associated with the control input. The term \mathcal{L}_{reg} serves as a regularization that suppresses excessively large control amplitudes and promotes smooth control trajectories, without defining the primary control objective. As indicated in Fig. 1, these loss components jointly guide the training process,

enabling the neural network to learn trajectories and controls that satisfy physical constraints while achieving the desired collective behavior.

The framework described above is independent of any specific dynamical model and applies broadly to nonlinear systems exhibiting collective dynamics. In the following sections, networked Kuramoto oscillators are adopted as a representative testbed, owing to their well-defined synchronization order parameter and their role as a standard benchmark for collective behavior. Importantly, the Kuramoto system serves only to instantiate the general physics-informed neural control framework introduced here, which is not restricted to this particular model.

III. INSTANTIATION ON NETWORKED KURAMOTO OSCILLATORS

To illustrate the general physics-informed neural control framework introduced in Sec. II, we consider a network of Kuramoto oscillators as a representative testbed. Owing to its simple phase dynamics and well-defined macroscopic order parameter, the Kuramoto model provides a canonical setting for investigating collective synchronization phenomena. Here, however, the Kuramoto system is employed solely to instantiate the general framework, rather than to delimit its applicability.

The dynamics of a network of N coupled phase oscillators are governed by

$$\dot{\theta}_i(t) = \omega_i + K \sum_{j=1}^N A_{ij} \sin(\theta_j(t) - \theta_i(t)) + u_i(t), \quad (5)$$

where $\theta_i(t) \in \mathbb{R}$ denotes the phase of oscillator i at time t , ω_i is its intrinsic natural frequency, K is the global coupling strength, and A_{ij} are the elements of the network adjacency matrix. The control input $u_i(t)$ enters additively into the phase dynamics and is learned within the physics-informed neural control framework. The collection of phases $\boldsymbol{\theta}(t) = (\theta_1(t), \dots, \theta_N(t))$ constitutes the system state appearing in Eq. (1).

Synchronization is characterized by the complex order parameter

$$R(t)e^{i\psi(t)} = \frac{1}{N} \sum_{j=1}^N e^{i\theta_j(t)}, \quad (6)$$

where $R(t) \in [0, 1]$ quantifies the instantaneous degree of phase coherence and $\psi(t)$ denotes the mean phase. Incoherent states correspond to values of $R(t)$ close to zero, whereas $R(t)$ approaching unity indicates strong synchronization. Within the present framework, the order parameter $R(t)$ serves as a macroscopic observable through which synchronization objectives are formulated.

Before introducing synchronization control, we verify that the physics-informed neural network can faithfully

represent the uncontrolled system dynamics across distinct dynamical regimes. A detailed validation of the PINN trajectory approximation, including both incoherent and spontaneously synchronized regimes of the Kuramoto model, is provided in Supplementary Sec. S1.

For a prescribed synchronization threshold $R^* \in (0, 1)$, the synchronization time is defined *a posteriori* as the trajectory-based quantity

$$T_s(R^*) = \inf \left\{ t \geq 0 \mid R(t') \geq R^*, \forall t' \geq t \right\}, \quad (7)$$

namely, the earliest time after which the order parameter remains above the threshold R^* . This definition excludes transient crossings and provides a robust characterization of synchronization onset in continuous time.

In the control formulation adopted here, synchronization requirements are specified instead through a *target time* t^* , which serves as a design parameter rather than a dynamical observable. The control objective is to enforce the inequality

$$T_s(R^*) \leq t^*, \quad (8)$$

that is, to require the system to have reached and maintained the prescribed synchronization level by the target time t^* . The synchronization time $T_s(R^*)$ itself is not directly optimized but is constrained implicitly through this requirement.

Within the physics-informed neural control framework, the phase trajectories $\theta_i(t)$ and control inputs $u_i(t)$ are parameterized using neural networks according to Eq. (2), while the Kuramoto dynamics in Eq. (5) are enforced through the physics-informed residual defined in Eq. (3). Synchronization objectives are incorporated by imposing a persistence constraint on the order parameter, requiring $R(t) \geq R^*$ for all $t \geq t^*$. In this way, both the synchronization level and the time at which it must be achieved are specified explicitly, without prescribing any explicit feedback control law.

For the Kuramoto testbed, the composite loss function introduced in Eq. (4) can be specified explicitly in terms of the phase variables and the synchronization order parameter. The dynamical loss enforcing consistency with Eq. (5) is defined as

$$\mathcal{L}_{\text{dyn}} = \frac{1}{N} \sum_{i=1}^N \left\langle \left| \frac{d\theta_i(t)}{dt} - \omega_i - K \sum_{j=1}^N A_{ij} \sin(\theta_j(t) - \theta_i(t)) - u_i(t) \right|^2 \right\rangle_t, \quad (9)$$

where $\langle \cdot \rangle_t$ denotes averaging over a set of collocation points in time.

The synchronization objective is imposed through a control loss constructed from the order parameter in Eq. (6). Given the prescribed threshold R^* and target time t^* , the synchronization loss is defined as

$$\mathcal{L}_{\text{control}} = \left\langle \mathbf{1}_{t \geq t^*} [\max(0, R^* - R(t))]^2 \right\rangle_{t \in [0, T]}, \quad (10)$$

where $\mathbf{1}_{t \geq t^*}$ denotes the indicator function. This formulation enforces the persistence condition $R(t) \geq R^*$ for all $t \geq t^*$ and thereby implements the constraint $T_s(R^*) \leq t^*$ within a differentiable, physics-informed optimization framework.

The initial condition loss enforcing the prescribed initial phases $\theta_i(0) = \theta_i^0$ is given by

$$\mathcal{L}_{\text{ic}} = \frac{1}{N} \sum_{i=1}^N |\theta_i(0) - \theta_i^0|^2, \quad (11)$$

and the control effort is regularized through a quadratic penalty on the control inputs,

$$\mathcal{L}_{\text{reg}} = \left\langle \frac{1}{N} \sum_{i=1}^N u_i(t)^2 \right\rangle_t, \quad (12)$$

which suppresses excessive control amplitudes and promotes smooth control trajectories.

We emphasize that \mathcal{L}_{reg} serves purely as a regularization term in the PINN training procedure and is not interpreted as a physical or performance metric. For reporting and comparison purposes, control effort is instead quantified *a posteriori* using the instantaneous control cost $P(t)$ and its time integral $E(t)$, introduced in Sec. IV A.

The accuracy of the physics-informed neural network in approximating uncontrolled dynamics is validated in the Supplementary Material.

In the following section, numerical results are presented to demonstrate the ability of the proposed framework to regulate synchronization dynamics in networked Kuramoto oscillators across a range of system parameters.

IV. NUMERICAL RESULTS

In this section, we present a series of numerical experiments to systematically validate the effectiveness and flexibility of the proposed physics-informed neural control framework for synchronization regulation. The numerical results are organized around three central aspects. First, we demonstrate that the framework can regulate the synchronization process in continuous time, including both the time required to reach synchronization and the achieved level of synchrony. Second, we investigate how the control cost required to enforce a given synchronization objective depends on intrinsic system parameters. Finally, we examine how the control cost varies with the synchronization targets themselves, namely the prescribed synchronization time and synchronization level.

Unless otherwise stated, all numerical experiments are performed on networked systems consisting of a moderate number of oscillators ($N = 10$), using the Kuramoto

phase model as a representative testbed. This choice allows the synchronization dynamics and the learned control signals to be clearly resolved and systematically analyzed, while avoiding unnecessary obscuration by high-dimensional state representations. The intrinsic frequencies and initial phases are randomly sampled from prescribed distributions, and the network topology and coupling strength are specified or scanned according to the purpose of each experiment. It is important to emphasize that the Kuramoto model is employed here solely as a concrete instantiation of the proposed framework, owing to its well-defined synchronization order parameter. The physics-informed neural control framework itself does not rely on any specific structural property of the Kuramoto dynamics and can, in principle, be extended to more general networked nonlinear dynamical systems. To assess scalability beyond the moderate system sizes considered in the main text, a representative demonstration at a larger network size is reported in the in Supplementary Sec. S3.

Synchronization is quantified using the order parameter $R(t)$, and the control objective is specified in terms of a target synchronization level R^* and a target time t^* , requiring the system to satisfy $R(t) \geq R^*$ for all $t \geq t^*$. Under this constraint, the physics-informed neural network simultaneously learns the system trajectories and the control inputs, such that the governing dynamics, synchronization requirements, and control cost are all satisfied within a unified optimization framework. In the following, we first present results for a representative baseline setting, and then analyze the dependence of the control cost on system parameters and synchronization targets.

A. Synchronization regulation under physics-informed neural control

In this subsection, we consider a representative baseline setting to illustrate the basic capability of the proposed physics-informed neural control framework for synchronization regulation. The purpose of this baseline experiment is not to exhaust the parameter space, but rather to demonstrate that, for a clearly specified synchronization objective, the framework can simultaneously regulate both the synchronization time and the synchronization level in continuous-time dynamics without prescribing an explicit control law.

Specifically, we consider a fully connected network of $N = 10$ oscillators. The intrinsic frequencies ω_i are independently drawn from a uniform distribution over the interval $[-\pi, \pi]$, while the initial phases $\theta_i(0)$ are sampled uniformly from the interval $[-\pi/2, \pi/2]$. The global coupling strength is fixed at $K = 0.05$. The synchronization objective is chosen to be complete synchronization, corresponding to a target synchronization level $R^* = 1$, together with a target time $t^* = 2$, such that the system is required to satisfy $R(t) \geq R^*$ for all $t \geq t^*$. Un-

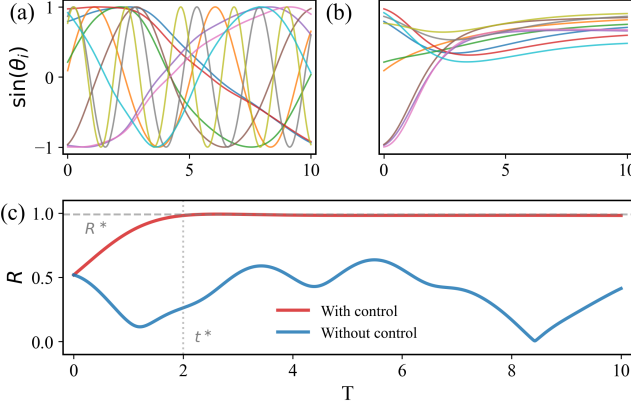


FIG. 2. (a) Phase time series of the oscillators without control, represented as $\sin \theta_i(t)$; (b) phase time series under physics-informed neural control; (c) time evolution of the order parameter $R(t)$ for controlled and uncontrolled dynamics. Dashed lines indicate the target synchronization level R^* and the target time t^* .

der this setting, the control input is allowed to act over the entire time interval, and no specific functional form of the control law is imposed a priori.

The dynamical evolution of the system in the absence and in the presence of physics-informed neural control is shown in Fig. 2. Without control, the phase time series of the oscillators, represented as $\sin \theta_i(t)$, remain dispersed and fail to exhibit coherent collective behavior, as illustrated in Fig. 2(a). In contrast, under physics-informed neural control, the phase trajectories gradually converge, leading to the formation of a synchronized state within a finite time, as shown in Fig. 2(b).

This difference is further clarified at the macroscopic level by the evolution of the order parameter. The time dependence of $R(t)$ for both controlled and uncontrolled dynamics is shown in Fig. 2(c), together with dashed lines indicating the target synchronization level R^* and the target time t^* . In the absence of control, the order parameter remains well below the target level throughout the time interval. By contrast, when control is applied, $R(t)$ increases rapidly and reaches $R^* = 1$ before t^* , after which it remains close to unity. These results demonstrate that the proposed framework enables precise regulation of both the synchronization time and the synchronization level in continuous time.

Having established that the synchronization objective is successfully achieved, we next examine the structure of the control signals learned by the physics-informed neural network. The time evolution of the control inputs $u_i(t)$ applied to individual oscillators is shown in Fig. 3(a). The control signals are continuous and smooth over the entire time horizon, with no evidence of impulsive or high-frequency behavior. As the system approaches the synchronized state, the magnitude of the control inputs decreases, indicating that only weak control is required to maintain synchronization once it has been established.

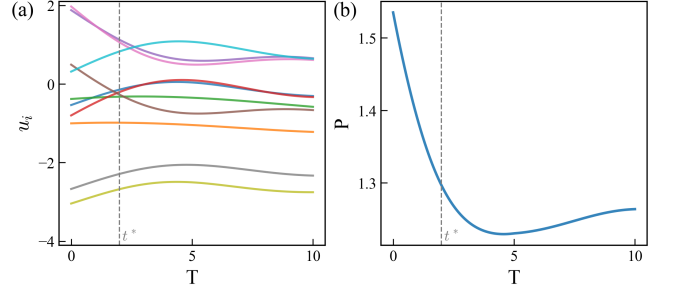


FIG. 3. (a) Time evolution of the control inputs $u_i(t)$ learned by the physics-informed neural network; (b) control cost density P as a function of time, quantifying the instantaneous control effort required to enforce the synchronization constraint.

To quantify the instantaneous control effort, we introduce the instantaneous control cost

$$P(t) = \frac{1}{N} \sum_{i=1}^N u_i^2(t), \quad (13)$$

which measures the magnitude of the applied control inputs at time t . This quantity is a dimensionless cost measure associated with control amplitudes and should not be interpreted as the physical power or energy of the oscillator network. As shown in Fig. 3(b), the control cost is relatively large during the synchronization formation stage and decreases substantially once the synchronized state is established, eventually approaching a steady value. This behavior indicates that the control action primarily facilitates the transient process leading to synchronization, while only a weak and sustained control effort is required to maintain the synchronized state thereafter.

To further illustrate this model independence, we apply the same framework to networks of Stuart–Landau oscillators, which include both amplitude and phase degrees of freedom; representative results are reported in the Supplementary Sec. S2.

B. Control cost under different conditions

In this subsection, we systematically investigate how the control expenditure required to achieve a prescribed synchronization objective depends on both intrinsic system properties and the specification of the control targets. Throughout this analysis, the network size and the physics-informed neural network (PINN) control framework are kept fixed, while different sources of synchronization difficulty are varied in a controlled manner. This allows us to quantitatively assess how distinct mechanisms that hinder synchronization are reflected in the required control cost.

To enable consistent comparisons across different con-

ditions, we define the integrated control cost as

$$E = \int_0^T P(t) dt, \quad (14)$$

where $P(t)$ denotes the instantaneous control cost defined in Eq. (13), and T is the terminal time of the control horizon. Due to the normalization by the network size N embedded in $P(t)$, the quantity $E(t)$ represents the average cumulative control effort per oscillator. This normalization ensures that variations in $E(t)$ can be directly interpreted as changes in synchronization difficulty rather than trivial scaling with system size.

We first examine the dependence of the integrated control cost on intrinsic system parameters while keeping the synchronization target (R^*, t^*) fixed, as shown in Fig. 4. Figure 4(a) reports the variation of $E(t)$ as a function of the frequency heterogeneity width δ , which characterizes the spread of intrinsic oscillator frequencies. As δ increases, the intrinsic frequencies become more broadly distributed, enhancing the tendency of the system to desynchronize. To compensate for this increased heterogeneity and enforce the same synchronization target, the controller must supply stronger and/or more persistent inputs, leading to a monotonic increase in the integrated control cost. This trend quantitatively captures the growing intrinsic difficulty of synchronizing a heterogeneous population of oscillators.

An opposite dependence is observed when varying the coupling strength K , as shown in Fig. 4(b). Increasing K enhances the effectiveness of mutual interactions in promoting phase alignment, thereby reducing the reliance on external control. Consequently, the integrated control cost decreases monotonically with increasing coupling strength. From a dynamical perspective, increasing K effectively counteracts frequency heterogeneity by strengthening collective synchronization tendencies. It is therefore natural that variations in K and δ lead to opposite trends in the control cost. The complementary behavior observed in Fig. 4 further supports the interpretation of $E(t)$ as a quantitative proxy for intrinsic synchronization difficulty.

We next investigate how the integrated control cost depends on the synchronization targets themselves, focusing on the required coherence level and the prescribed synchronization time. The quantity $E(t)$ defined in Eq. (14) provides a direct measure of the cumulative effort needed to meet a given control objective.

We first consider the dependence of $E(t)$ on the target synchronization level R^* while keeping the target time t^* fixed. As R^* increases, the integrated control cost grows monotonically and rises sharply as R^* approaches unity. This behavior reflects the increasing difficulty of enforcing near-complete phase coherence: achieving higher synchronization accuracy requires progressively finer phase alignment, which in turn demands stronger and more sustained control actions to suppress residual phase fluctuations.

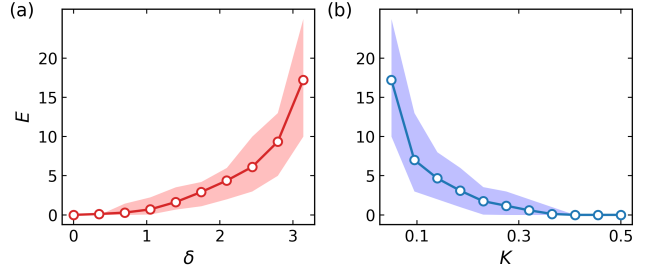


FIG. 4. Integrated control cost $E(t)$ under different intrinsic system conditions. (a) Dependence of $E(t)$ on the frequency heterogeneity width δ . (b) Dependence of $E(t)$ on the coupling strength K . In both panels, the synchronization target (R^*, t^*) and all other system parameters are fixed. Solid lines indicate mean values, while shaded regions represent variability across independent realizations; for each parameter value, results are averaged over 20 independent runs with different random initial conditions and frequency realizations.

We then examine the complementary dependence of $E(t)$ on the target synchronization time t^* , with the synchronization level R^* held fixed. In this case, the integrated control cost decreases systematically as t^* increases. Enforcing synchronization within a shorter time window requires more aggressive control interventions to accelerate convergence toward the synchronized manifold, thereby increasing the cumulative control cost. Allowing a longer synchronization time enables the intrinsic coupling dynamics to contribute more effectively, reducing the burden on external control.

Across the entire parameter range considered, the variability of the integrated control cost over repeated training runs remains moderate, indicating that the observed trends are robust with respect to stochastic effects associated with random initial conditions and neural network optimization.

Overall, these results reveal a clear trade-off between synchronization performance and control expenditure: achieving higher coherence or faster convergence inevitably incurs higher control cost. By explicitly quantifying this trade-off within a continuous-time, physics-informed framework, the proposed approach provides a principled tool for exploring cost–performance landscapes in synchronization regulation problems.

C. Comparison with baseline strategies

In this subsection, we benchmark the proposed physics-informed neural network (PINN) control framework against representative baseline strategies for synchronization regulation, with particular emphasis on control energy efficiency. Rather than aiming to solve an optimal control problem in a strict theoretical sense, the goal of this comparison is to assess whether the PINN-based framework can systematically identify low-energy

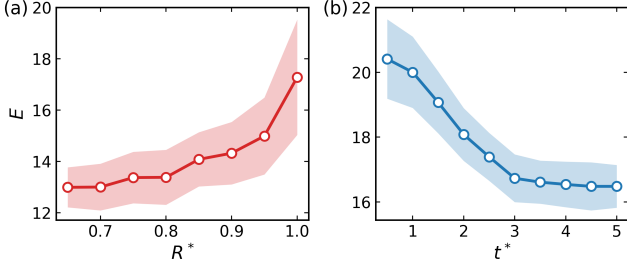


FIG. 5. Dependence of the integrated control cost $E(t)$ on synchronization targets. (a) Integrated control cost as a function of the target synchronization level R^* with fixed target time t^* . (b) Integrated control cost as a function of the target synchronization time t^* with fixed R^* . Solid lines denote mean values over 20 independent runs, and shaded regions indicate the corresponding variability.

admissible control trajectories under identical dynamical constraints and synchronization objectives. All methods are evaluated under the same system parameters, and the comparison focuses on both transient control behavior, quantified by the instantaneous control cost $P(t)$, and cumulative control expenditure, quantified by the integrated control cost $E(t)$.

We consider three commonly used baseline strategies: linear phase-based feedback, nonlinear (sinusoidal) phase-based feedback, and frequency-based compensation. The linear phase-based control is given by

$$u_i(t) = -k_\theta(\theta_i(t) - \bar{\theta}(t)), \quad (15)$$

while the nonlinear phase-based control takes the form

$$u_i(t) = -k_\theta \sin(\theta_i(t) - \bar{\theta}(t)), \quad (16)$$

where $\bar{\theta}(t)$ denotes the instantaneous mean phase. In contrast, the frequency-based strategy compensates intrinsic frequency heterogeneity via

$$u_i(t) = -k_\omega(\omega_i - \bar{\omega}), \quad (17)$$

with $\bar{\omega}$ being the mean intrinsic frequency. For the Kuramoto model, this compensation strategy admits an analytic solution and therefore serves as a natural *analytical reference* for assessing energy efficiency within additive control schemes, rather than as a universal optimality benchmark.

For each baseline method, the control gain is selected by scanning the corresponding parameter space and choosing the minimal value that reliably yields a synchronized state with $R \simeq 1$. As indicated by the inset parameter scans in Fig. 6(a), phase-based feedback requires a gain of $k_\theta = 1.5$, whereas frequency-based compensation achieves synchronization already at $k_\omega = 1$. These values are used consistently throughout the comparison to ensure identical synchronization performance and a fair assessment of transient behavior and control cost.

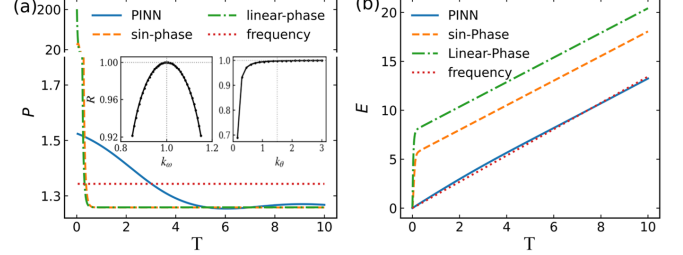


FIG. 6. Benchmark comparison between PINN-based control and baseline strategies in the Kuramoto model. (a) Instantaneous control cost $P(t)$. (b) Integrated control cost $E(t)$.

The temporal evolution of the instantaneous control cost $P(t)$ reveals a clear qualitative distinction between the PINN-based control and the phase-based baselines, as shown in Fig. 6(a). Both linear and nonlinear phase feedback exhibit pronounced transient peaks at early times, reflecting their strong sensitivity to the initial phase configuration. When oscillators are initially far from coherence, large corrective inputs are required to rapidly suppress phase dispersion, resulting in abrupt and intense control actions. Such transient behavior may pose practical limitations in systems subject to actuator saturation or amplitude constraints.

By contrast, the PINN-based control produces smooth and gradually varying control profiles without sharp transients. By explicitly incorporating the governing dynamics and synchronization objectives during training, the PINN distributes control effort more evenly over time, thereby biasing the learned trajectories toward energy-efficient admissible solutions rather than aggressively correcting instantaneous phase deviations.

The accumulated control cost further highlights the differences between control strategies. As shown in Fig. 6(b), both phase-based feedback schemes incur substantially larger integrated control cost, dominated by their large early-time transients. In this analytically tractable setting, frequency-based compensation provides a meaningful low-energy reference. Remarkably, the cumulative control cost achieved by the PINN is found to be comparable to this analytical reference, despite the absence of any explicitly prescribed frequency-compensation control law. This observation indicates that the PINN-based framework is capable of discovering highly energy-efficient control trajectories directly from the governing dynamics, without invoking optimal control formulations or analytic solutions.

The above comparison relies on the existence of an analytically solvable frequency-compensation strategy, which is specific to gradient synchronization dynamics such as the Kuramoto model. In such systems, intrinsic frequency heterogeneity can be compensated analytically, providing a meaningful low-energy reference for additive control schemes. However, this type of analytical baseline ceases to exist once the underlying gradient structure is broken.

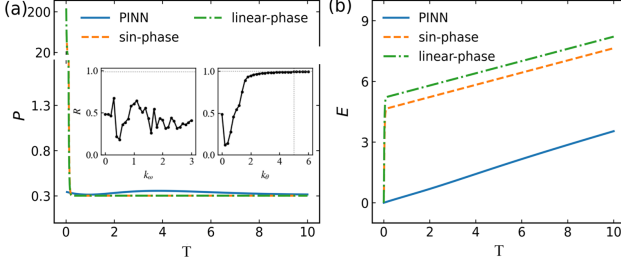


FIG. 7. Benchmark comparison between PINN-based control and baseline strategies in the Kuramoto-Sakaguchi model. (a) Instantaneous control cost $P(t)$. (b) Integrated control cost $E(t)$.

To assess the robustness of the proposed physics-informed neural network (PINN) control framework beyond gradient systems and to illustrate the limitations of analytical references, we consider the Kuramoto-Sakaguchi model,

$$\dot{\theta}_i(t) = \omega_i + K \sum_{j=1}^N \sin(\theta_j(t) - \theta_i(t) - \alpha) + u_i(t), \quad (18)$$

where the phase lag α introduces intrinsic frustration. This phase shift breaks the potential structure underlying the Kuramoto model and renders the dynamics non-gradient, thereby eliminating the analytical tractability of frequency-based compensation strategies.

The control performance in a representative frustrated regime with $\alpha = \pi/2$ and coupling strength $K = 0.4$ is summarized in Fig. 7. In this regime, the uncontrolled system does not admit a synchronized state with $R \approx 1$, and frequency-based compensation fails to stabilize synchronization, thereby ceasing to provide a meaningful reference. This breakdown is reflected in both the instantaneous and accumulated control costs shown in Fig. 7(a,b).

Phase-based feedback can still enforce synchronization under these non-gradient dynamics. However, as shown in Fig. 7(a), this is achieved at the expense of pronounced transient peaks in the instantaneous control cost $P(t)$, arising from the strong sensitivity of phase feedback to instantaneous phase dispersion. These early-time peaks dominate the accumulated control cost, leading to a substantially larger integrated control cost $E(t)$, as shown in Fig. 7(b).

By contrast, the PINN-based framework remains effective in this frustrated regime. The learned control signals yield smooth temporal profiles without sharp transients, resulting in consistently reduced instantaneous control cost and a significantly lower integrated control cost compared to phase-based feedback. Importantly, this improvement is achieved without relying on any analytic structure specific to gradient systems.

This comparison highlights the methodological advantage of the physics-informed neural control framework. Rather than exploiting problem-specific analytical prop-

erties, the PINN performs a physics-constrained search over admissible control trajectories and is naturally biased toward low-energy solutions through its training objective. As a result, the framework provides a flexible and energy-efficient control discovery mechanism that remains effective even in frustrated and non-gradient synchronization dynamics, where conventional analytical baselines and optimality notions are no longer available.

D. Robustness to noise

In practical applications, synchronization control is inevitably affected by stochastic perturbations arising from environmental fluctuations, unmodeled dynamics, or measurement uncertainty. It is therefore essential to assess whether the proposed physics-informed neural network (PINN) control strategy can maintain stable synchronization under noisy conditions, despite being designed as an offline trajectory-level controller.

To this end, we examine the robustness of the learned control signals by introducing additive stochastic perturbations into the controlled Kuramoto dynamics during the *execution stage*, while keeping the PINN-trained control inputs fixed. Specifically, after training the PINN under deterministic dynamics, the system is evolved according to the stochastic differential equation

$$\dot{\theta}_i(t) = \omega_i + K \sum_{j=1}^N A_{ij} \sin(\theta_j(t) - \theta_i(t)) + u_i(t) + \sigma \xi_i(t), \quad (19)$$

where $\xi_i(t)$ denotes independent Gaussian white noise satisfying $\langle \xi_i(t) \rangle = 0$ and $\langle \xi_i(t) \xi_j(t') \rangle = \delta_{ij} \delta(t - t')$. The parameter σ controls the noise intensity. Unless otherwise stated, the control signals $u_i(t)$ are those learned from noiseless PINN training and are not adapted online.

The robustness of the PINN-based control is quantified using three complementary metrics: (i) the time-averaged order parameter $\langle R \rangle = (T - t^*)^{-1} \int_{t^*}^T R(t) dt$, (ii) the relative synchronization error $\mathcal{E}_R = (R^* - \langle R \rangle)/R^*$, and (iii) the integrated control cost $E(t)$. For each noise intensity σ , all quantities are averaged over multiple independent noise realizations.

Figure 8(a) shows the dependence of synchronization performance on the noise intensity σ for a fixed coupling strength and a target synchronization level $R^* = 1$. As σ increases, the time-averaged order parameter $\langle R \rangle$ decreases gradually from unity, indicating a progressive degradation of phase coherence induced by stochastic perturbations. At the same time, the synchronization error \mathcal{E}_R increases monotonically with σ , reflecting enhanced fluctuations around the synchronized manifold rather than an abrupt loss of global synchronization. Importantly, synchronization remains robust over a broad range of noise intensities, with $\langle R \rangle$ staying close to unity even for moderately strong noise.

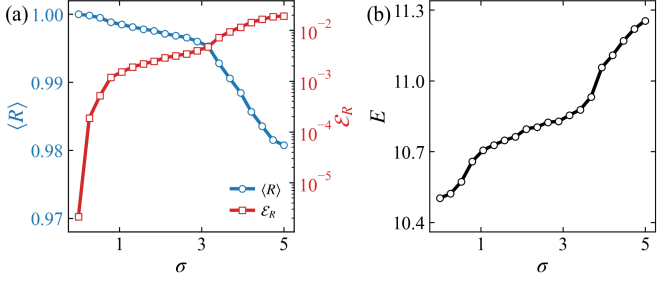


FIG. 8. Noise robustness analysis of the PINN-controlled system. (a) Time-averaged order parameter $\langle R \rangle$ (left axis) and relative synchronization error \mathcal{E}_R (right axis) as functions of the noise intensity σ for a fixed coupling strength and target $R^* = 1$. (b) Integrated control cost $E(t)$ as a function of the noise intensity σ under the same noisy conditions.

The corresponding variation of the integrated control cost $E(t)$ as a function of the noise intensity σ is reported in Fig. 8(b). Because the control inputs are fixed offline and not adjusted in response to instantaneous noise realizations, the overall magnitude of $E(t)$ remains finite and varies smoothly with increasing σ . The observed increase in $E(t)$ reflects the additional control effort required to suppress noise-induced phase fluctuations and to stabilize the collective dynamics against stronger stochastic perturbations.

Taken together, these results demonstrate that the PINN-based control strategy exhibits inherent robustness to stochastic perturbations. Rather than reacting aggressively to instantaneous noise realizations, the learned control stabilizes synchronization at a global, trajectory level, ensuring that macroscopic coherence is maintained with only a modest and smoothly varying increase in control cost. This robustness, achieved without online feedback or adaptive re-optimization, underscores the practical viability of the proposed physics-informed control framework in noisy environments.

V. DISCUSSION

The results presented in this work establish physics-informed neural networks (PINNs) as an effective and flexible framework for continuous-time synchronization regulation in networked nonlinear dynamical systems. Beyond demonstrating the realization of prescribed synchronization objectives in the Kuramoto testbed, the primary contribution of this study is methodological: synchronization control is reformulated as a unified, physics-constrained, trajectory-level optimization problem, in which admissible system trajectories and control inputs are learned simultaneously while macroscopic synchronization requirements are imposed explicitly in time.

A key conceptual distinction between the proposed PINN-based framework and conventional synchronization control strategies lies in the nature of the learned object. Rather than prescribing an explicit feedback

law or control structure *a priori*, the PINN parameterizes entire state and control trajectories over a finite time horizon and enforces dynamical consistency through physics-informed residuals. From this perspective, training the PINN can be interpreted as solving an implicit continuous-time constrained optimization problem: among all trajectories that satisfy the governing equations and synchronization constraints, those minimizing a prescribed control regularization are selected. As a result, the learned control does not correspond to a local-in-time reaction to instantaneous phase deviations, but instead represents a globally optimized intervention profile that distributes control effort coherently across time. This global-in-time character naturally explains the smooth temporal structure of the learned control signals and the absence of impulsive or high-frequency components.

The systematic comparison with phase-based baseline strategies highlights an intrinsic limitation of instantaneous phase feedback. Both linear and nonlinear phase-feedback controls act directly on deviations from the instantaneous mean phase. When the initial phase configuration is highly incoherent, large phase dispersion leads to strong corrective forces at early times, resulting in pronounced transient peaks in the instantaneous control cost. These peaks are not numerical artifacts but arise from the fundamental sensitivity of phase-based feedback to initial conditions and instantaneous phase geometry. In practical scenarios involving actuator saturation, amplitude constraints, or power limitations, such large transient demands may significantly restrict the applicability of purely phase-based control schemes, even when synchronization can eventually be achieved.

The frequency-compensation baseline occupies a distinct conceptual role. For the Kuramoto model, compensating intrinsic frequency heterogeneity constitutes an analytically tractable strategy and provides a meaningful reference for assessing control efficiency in this specific gradient system. The observation that the integrated control cost achieved by the PINN-based approach closely matches that of frequency compensation admits a clear interpretation: by exploiting the governing dynamics together with explicit synchronization constraints during training, the PINN is able to identify a control trajectory that is effectively near-optimal for this analytically solvable case, without explicitly encoding the corresponding control law. Importantly, this agreement should be viewed as a validation of the framework in a setting where a theoretical benchmark exists, rather than as evidence of any universal optimality guarantee. For more general nonlinear or non-gradient systems, analytic frequency-based controls are typically unavailable, whereas the PINN formulation remains directly applicable.

This distinction becomes particularly relevant in frustrated or non-gradient dynamics, such as the Kuramoto-Sakaguchi model examined in this work. In such settings, frequency-based compensation ceases to provide a mean-

ingful baseline, and phase-based feedback often incurs substantially increased transient and cumulative control costs. By contrast, the PINN-based framework continues to produce smooth and effective synchronization control, underscoring that its performance does not rely on special gradient structures of the underlying dynamics. This robustness to the qualitative nature of the dynamical system highlights the generality of the physics-informed trajectory optimization perspective.

The applicability of the framework is further supported by the extensions reported in the Supplementary Material. In particular, the successful application to networks of Stuart–Landau oscillators demonstrates that the approach naturally extends beyond pure phase models to systems with both amplitude and phase degrees of freedom. This confirms that the framework does not rely on specific properties of the Kuramoto order parameter but instead applies whenever a suitable macroscopic collective observable can be defined. Moreover, representative demonstrations at larger network sizes indicate that the approach remains feasible beyond the small systems used for detailed analysis in the main text. While increasing system size raises representational and optimization demands, these challenges are primarily technical rather than conceptual and can be addressed by increasing network capacity, refining collocation strategies, and leveraging parallel computation.

An additional advantage of the PINN formulation lies in the explicit manner in which synchronization objectives are specified and enforced. In conventional approaches, control laws are designed first and synchronization performance—both in terms of coherence level and convergence time—is assessed *a posteriori*. In contrast, the PINN framework incorporates macroscopic synchronization requirements directly into the continuous-time learning objective. Targets specifying both the desired synchronization level and the time at which it must be reached and maintained are imposed explicitly within the optimization problem, rendering synchronization performance a programmable specification rather than an emergent byproduct of a chosen feedback structure.

Several limitations of the present study should be acknowledged. The current implementation constitutes an offline design procedure: the learned control corresponds to a trajectory optimized for a given objective and set of conditions, rather than a real-time adaptive feedback controller. Training costs increase with system dimension and with the strictness of imposed constraints, and robustness to model mismatch is not explicitly addressed. These limitations are largely practical in nature. Future work may explore hybrid strategies that combine physics-informed trajectory optimization with structured feed-

back, extensions to systems with explicit actuator constraints or uncertainties, and online or adaptive variants of the framework to enhance robustness and real-time applicability.

VI. CONCLUSION

In this work, we have proposed a physics-informed neural network (PINN) framework for continuous-time synchronization regulation in networked nonlinear dynamical systems. By jointly parameterizing system trajectories and control inputs within a unified neural representation and explicitly enforcing the governing dynamics, synchronization objectives, and control regularization during training, the proposed approach enables direct regulation of both the synchronization level and the time scale over which coherence emerges.

Using networked Kuramoto oscillators as a representative testbed, we demonstrated that the PINN-based control achieves smooth synchronization without impulsive transients and attains a cumulative control cost that closely approaches the efficiency of analytically motivated frequency-compensation strategies in gradient dynamics, while avoiding the large early-time power peaks characteristic of phase-based feedback. Importantly, the framework remains effective in non-gradient and frustrated settings, where conventional baselines lose their theoretical justification.

Beyond the specific numerical examples, the principal contribution of this work is methodological. By embedding macroscopic synchronization requirements directly into a continuous-time, physics-constrained optimization problem, the PINN framework transforms synchronization regulation into a programmable design task. Trade-offs between synchronization accuracy, convergence time, and control expenditure can be explored systematically without prescribing explicit control laws.

The Supplementary Material further demonstrates the generality of the approach, including extensions to limit-cycle oscillators with amplitude dynamics and representative scalability to larger network sizes. While practical challenges remain in terms of computational cost and offline implementation, the framework is broadly applicable to networked systems governed by ordinary differential equations, provided suitable collective observables can be defined.

Taken together, these results position physics-informed neural control as a promising and versatile tool for the regulation of collective dynamics, offering a unified perspective that bridges dynamical systems theory, optimal control, and machine learning.

[1] A. Pikovsky, M. Rosenblum, and J. Kurths, *Synchronization: A Universal Concept in Nonlinear Sciences* (Cambridge University Press, 2001).

[2] S. H. Strogatz, *Sync: The Emerging Science of Spontaneous Order* (Hyperion, 2003).

[3] K. Wiesenfeld, P. Colet, and S. H. Strogatz, Synchronization

tion of josephson-junction arrays, *Physical Review E* **54**, 1563 (1996).

[4] M. C. Soriano, J. García-Ojalvo, C. R. Mirasso, and I. Fischer, Complex photonics: Dynamics and applications of delay-coupled semiconductors lasers, *Reviews of Modern Physics* **85**, 421 (2013).

[5] G. Buzsáki, *Rhythms of the Brain* (Oxford University Press, 2006).

[6] F. Dörfler, M. Chertkov, and F. Bullo, Synchronization in complex oscillator networks and smart grids, *Proceedings of the National Academy of Sciences* **110**, 2005 (2013).

[7] Y. Kuramoto, *Chemical Oscillations, Waves, and Turbulence* (Springer-Verlag, 1984).

[8] E. Schöll and H. G. Schuster, *Handbook of Chaos Control* (John Wiley & Sons, 2008).

[9] A. Arenas, A. Díaz-Guilera, J. Kurths, M. Moreno, and C. Zhou, Synchronization in complex networks, *Physics Reports* **469**, 93 (2008).

[10] X.-F. Wang and F. Xiao, Finite-time synchronization of complex networks, *IEEE Transactions on Circuits and Systems I: Regular Papers* **57**, 2114 (2010).

[11] J. Lu, D. W. Ho, J. Cao, and J. Kurths, Finite-time synchronization of complex networks with time-varying delays, *Pramana* **80**, 121 (2013).

[12] D. M. Abrams and S. H. Strogatz, Chimera states for coupled oscillators, *Physical Review Letters* **93**, 174102 (2004).

[13] V. N. Belykh, I. V. Belykh, and M. Hasler, Cluster synchronization in oscillatory networks, *Physical Review E* **69**, 056205 (2004).

[14] K. Luo, Z. Cai, Z. Liu, S. Guan, and Y. Zou, Effects of uncommon non-isochronicities on remote synchronization, *Chaos, Solitons & Fractals* **181**, 114705 (2024).

[15] P. S. Skardal and A. Arenas, Control of coupled oscillator networks with external forcing, *Science Advances* **1**, e1500339 (2015).

[16] A. Zlotnik, Y.-C. Chen, I. Z. Kiss, J.-S. Lin, and J.-S. Li, Optimal control of entrainment in networks of coupled oscillators, *Physical Review Letters* **111**, 024102 (2013).

[17] M. G. Rosenblum and A. S. Pikovsky, Controlling synchronization in an ensemble of globally coupled oscillators, *Physical Review Letters* **92**, 114102 (2004).

[18] X. F. Wang and G. Chen, Pinning control of scale-free dynamical networks, *Physica A: Statistical Mechanics and its Applications* **310**, 521 (2002).

[19] X. Li, X. F. Wang, and G. Chen, Pinning control of complex network groups with small-world connectivity, *Physica A: Statistical Mechanics and its Applications* **332**, 584 (2004).

[20] G. Chen, Pinning control and controllability of complex dynamical networks, *International Journal of Bifurcation and Chaos* **17**, 4101 (2007).

[21] H. K. Khalil, *Nonlinear Systems* (Prentice Hall, 2002).

[22] J. Sun, E. M. Boltt, and T. Nishikawa, Synchronization of heterogeneous oscillator networks, *EPL (Europhysics Letters)* **85**, 60011 (2009).

[23] A. E. Motter, S. A. Myers, M. Anghel, and T. Nishikawa, Spontaneous synchrony in power-grid networks, *Nature Physics* **9**, 191 (2013).

[24] Y. Tang, H. Gao, W. Zou, and J. Kurths, Synchronization in complex networks and its application—a survey, *International Journal of Control* **87**, 917 (2014).

[25] M. Raissi, P. Perdikaris, and G. E. Karniadakis, Physics-informed neural networks: A deep learning framework for solving forward and inverse problems involving nonlinear partial differential equations, *Journal of Computational Physics* **378**, 686 (2019).

[26] K. Luo, Variational physics-informed ansatz for reconstructing hidden interaction networks from steady states (2025), arXiv:2512.13708 [cs.LG].

[27] G. E. Karniadakis, I. G. Kevrekidis, L. Lu, P. Perdikaris, S. Wang, and L. Yang, Physics-informed machine learning, *Nature Reviews Physics* **3**, 422 (2021).

[28] L. Lu, X. Meng, Z. Mao, and G. E. Karniadakis, Deepxde: A deep learning library for numerical differential equations, *SIAM Review* **63**, 208 (2021).

[29] E. A. Antonelo *et al.*, Physics-informed neural nets for control of dynamical systems, arXiv preprint arXiv:2104.02556 (2021).

[30] C. Rackauckas *et al.*, Universal differential equations for scientific machine learning, arXiv preprint arXiv:2001.04385 (2020).

[31] Y. Chen *et al.*, Enhanced physics-informed neural networks (pinns) for high-order power grid dynamics, arXiv preprint arXiv:2410.10110 (2024).

[32] S. Mowlavi and L. Mahadevan, Optimal control of self-organization in active matter using physics-informed neural networks, *Scientific Reports* **13**, 11174 (2023).